Modulational instability of a trapped Bose-Einstein condensate with two- and three-body interactions

Etienne Wamba,[1,*] Alidou Mohamadou,[1,2,†] and Timoléon C. Kofané[1,‡]
[1]*Laboratory of Mechanics, Department of Physics, Faculty of Science, University of Yaounde I, P. O. Box 812, Yaounde, Cameroon*
[2]*Condensed Matter Laboratory, Department of Physics, Faculty of Science, University of Douala, P. O. Box 24157, Douala, Cameroon*
(Received 7 August 2007; revised manuscript received 8 January 2008; published 23 April 2008)

We investigate analytically and numerically the modulational instability of a Bose-Einstein condensate with both two- and three-body interatomic interactions and trapped in an external parabolic potential. Analytical investigations performed lead us to establish an explicit time-dependent criterion for the modulational instability of the condensate. The effects of the potential as well as of the quintic nonlinear interaction are studied. Direct numerical simulations of the Gross-Pitaevskii equation with two- and three-body interactions describing the dynamics of the condensate agree with the analytical predictions.

DOI: 10.1103/PhysRevE.77.046216 PACS number(s): 05.45.Yv, 03.75.Lm, 42.65.Sf, 03.75.Kk

I. INTRODUCTION

Bose-Einstein condensation (BEC) is a ubiquitous phenomenon that plays a significant role in condensed matter, atomic, nuclear, and elementary particle physics, as well as in astrophysics [1]. Its most striking feature is a macroscopic population of the ground state of the system at finite temperature [2]. The study of BEC in weakly interacting systems holds the promise of revealing new macroscopic quantum phenomena that can be understood from first principles, and may also advance our understanding of superconductivity and superfluidity in more complex systems. The spatial contraction of wave packets and the formation of a singularity in finite time, wave collapse or, more generally, the blowup of the wave packet are basic phenomena in nonlinear physics of wave systems. Examples are the self-focusing of light in optics [3,4], the collapse of Langmuir waves in plasma [5], the self-focusing of gravity-capillary surface waves [6], the blowup of nonlinear electronic excitations in molecular systems [7], and collapse in a Bose gas with negative scattering length. There have been several theoretical studies on different aspects of BEC in one- [8–10] as well as three-dimensional [10,11] optical-lattice potentials combined with axially symmetric harmonic ones.

Progress with BEC on the surface of atomic chips and atomic waveguides involves a strong compression of the BEC and an essential increase of its density. Then the problem arises of taking into account three-body interaction effects, corresponding to a quintic mean-field nonlinearity. This interaction is interesting also for an understanding of the fundamental limits of the functioning of BEC-based devices [12]. The existence of three-body interactions can play an important role in condensate stability [13,14]. Recently, three-body interactions arising due to the Efimov resonance were observed in an ultracold gas of cesium atoms [15]. Thus it is interesting to investigate the properties of discrete breathers in BECs in optical lattices when two- and three-body interactions are taken into account. One important property of this system is the existence of gap-Townes solitons [16,17] and the essential modification of energy band properties by the three-body interaction [18]. In the tight-binding approximation, the Gross-Pitaevskii (GP) equation with two- and three-body interactions and a periodic potential can be reduced to the cubic-quintic discrete nonlinear Schrödinger (CQDNLS) equation. This regime, realized in typical experiments with BECs [19], occurs for a deep optical lattice. The GP equation with cubic and quintic nonlinearities also appears in the description of the evolution of a broad gap soliton under the joint action of linear and nonlinear optical lattices. If the nonlinear optical lattice rapidly varies in space in comparison with the periodic potential one, averaging the GP equation over this modulation leads to the appearance of an effective quintic nonlinearity [20,21].

An important aspect of the investigation is the underlying physical mechanism of BEC solitary waves, since it is believed that the generation and evolution of BEC solitary waves is important for a number of BEC applications, such as atomic interferometry [22] and different kinds of quantum phase transitions [23], as well as in the context of nonlinear physics, including nonlinear optics and hydrodynamics. In the relevant experiments, bright solitons have been created by changing the *s*-wave scattering length from positive to negative [9]. On the other hand, it was shown that bright solitary wave structures may appear by the activation of a modulational instability (MI) of plane waves [24]. In this case, the continuous wave solution becomes unstable toward the generation of a chain of bright solitons.

The formation of localized, coherent solitary wave structures, i.e., localization in position space, is equivalent to delocalization in momentum space. It is a result of modulational instability [24–28] for which, a specific range of wave numbers of plane-wave profiles becomes unstable to modulations, leading to an exponential growth of the unstable modes and eventually to that delocalization [26–28]. MI is a general feature of continuum as well as discrete nonlinear matter-wave equations and has been both experimentally and theoretically established as responsible for not only the position space localization but also dephasing. In the present work, we reconsider theoretically and numerically the MI for

*wambaetienne@yahoo.fr
†mohdoufr@yahoo.fr
‡tckofane@yahoo.com

a trapped BEC immersed in a highly elongated harmonic trap, considering both two- and three-body interactions. Our interest is to derive an explicit time-dependent criterion for MI for such a system. With this aim, we perform a modified lens-type transformation which converts our initial GP equation, with real position-dependent parabolic potential and constant coefficients of nonlinearity, into a GP equation without potential and with a constant coefficient of quintic nonlinearity and a time-dependent coefficient of cubic nonlinearity. The work is organized as follows In Sec. II, we present the mathematical framework and the MI in the CQNLS equation as well as the stability regions of the wave in the lattice. Then in Sec. III, we perform a direct numerical integration of the initial one-dimensional (1D) GP equation to study the MI numerically. The results obtained are compared to those of the analytical treatment and excellent agreement is found. Section IV is devoted to conclusion.

II. GENERAL CONSIDERATIONS AND ANALYTICAL RESULTS

The system, a BEC trapped in a harmonic potential in the presence of two- and three-body interatomic interactions, can be described by a quasi-1D GP equation, which has the form of a CQNLS equation, written in the normalized form [16]

$$i\psi_t = -\psi_{xx} + V(x)\psi + g_0|\psi|^2\psi + \chi|\psi|^4\psi, \tag{1}$$

where ψ is the normalized macroscopic wave function. $V(x)=\alpha x^2$ is the external harmonic (magnetic) potential which will be taken as attractive [25], i.e., the trapping coefficient α (a real constant here) is positive. g_0 and χ are, respectively, the two- and three-body interaction coefficients, positive for repulsive interatomic interactions and negative for attractive ones [29]. Such an equation also serves as a mean-field model in the description of the dynamics of a cigar-shaped BEC with repulsive interatomic interactions trapped in the potential $V(x)$ [30]. The CQNLS equation appears in the context of nonlinear photonic crystals [16,31]. This equation is also used as a model for the propagation of optical pulses in double-doped optical fibers with an effective refractive index [16,32]. When the cubic nonlinearity term is absent, the resultant equation is a model for the dynamics of the Bose gas with hard-core interactions in the Tonks-Girardeau regime [25,16,33].

For MI investigations in a BEC, let us first perform a modified lens-type transformation. For this, we set [25]

$$\psi(x,t) = \frac{1}{\sqrt{\ell(t)}}\phi(X,T)\,\exp[if(t)x^2], \tag{2}$$

in which we choose $\ell(t)=|\cos(2\sqrt{\alpha}t)|$, $X=\frac{x}{\ell(t)}$, $T(t)=\frac{1}{2\sqrt{\alpha}}\tan(2\sqrt{\alpha}t)$, and $f(t)=-\frac{\sqrt{\alpha}}{2}\tan(2\sqrt{\alpha}t)$. The rescaling signals singularity at any $t\neq\frac{(2n+1)\pi}{4\sqrt{\alpha}}$ (n is a positive integer) in the (t,T) domain and the possibility for T to be negative. We focus our study on the case where t goes from zero to $\frac{\pi}{4\sqrt{\alpha}}$ to guarantee that T goes from zero to infinity. Then Eq. (1), in terms of rescaled variables X and T, is reduced to

$$i\phi_T = -\phi_{XX} + g(T)|\phi|^2\phi + \chi|\phi|^4\phi, \tag{3}$$

where $g(T)=g_0(1+4\alpha T^2)^{-1/2}$. This rescaled equation has the form of a CQNLS equation with a time-dependent coefficient and, importantly, without a potential.

In order to examine the MI of the BEC, we use the ansatz

$$\phi = (\phi_0 + \delta\phi)\exp\left(-i\int_0^T \Omega(v)dv\right), \tag{4}$$

where $\Omega(T)$ is a real time-dependent function representing the nonlinear frequency shift, ϕ_0 is a real constant, and $\delta\phi$ is the amplitude perturbation. Substituting Eq. (4) into Eq. (3), neglecting second-order terms in $\delta\phi$ and its complex conjugate $\delta\phi^*$, we take

$$\Omega(T) = \phi_0^2[g(T) + \chi\phi_0^2], \tag{5}$$

to obtain the following equation describing the dynamics of the perturbation:

$$i\frac{\partial\delta\phi}{\partial T} = -\frac{\partial^2\delta\phi}{\partial X^2} + \Delta(T)(\delta\phi + \delta\phi^*). \tag{6}$$

In Eq. (6), $\Delta(T)=\phi_0^2[g(T)+2\chi\phi_0^2]$. Let u_1 and u_2 be, respectively, the real and imaginary parts of $\delta\phi$. Then Eq. (6) is transformed into the following two coupled equations:

$$\frac{\partial u_1}{\partial T} + \frac{\partial^2 u_2}{\partial X^2} = 0, \tag{7}$$

$$-\frac{\partial u_2}{\partial T} + \frac{\partial^2 u_1}{\partial X^2} - 2\Delta(T)u_1 = 0. \tag{8}$$

Now, we consider that the variation of the perturbation obeys the expression:

$$u_1 = \mathrm{Re}\left\{U_1\exp\left[i\left(KX - \int_0^T \omega(v)dv\right)\right]\right\}$$

and

$$u_2 = \mathrm{Im}\left\{U_2\exp\left[i\left(KX - \int_0^T \omega(v)dv\right)\right]\right\}, \tag{9}$$

where $KX-\int_0^T\omega(v)dv$ is the modulation phase in which K and ω are, respectively, the wave number and frequency of the modulation. After some calculations, we obtain the following explicitly time-dependent dispersion relation:

$$\omega^2 = K^4\left[1 + 2\left(\frac{\phi_0}{K}\right)^2(g_0(1+4\alpha T^2)^{-1/2} + 2\chi\phi_0^2)\right]. \tag{10}$$

For the MI to arise, the frequency of modulation must be complex with non-nil imaginary part. Such a condition may be simply realized if the right-hand side of Eq. (10) is negative; that is,

$$2g_0\left(\frac{\phi_0}{K}\right)^2(1+4\alpha T^2)^{-1/2} + 4\chi\phi_0^2\left(\frac{\phi_0}{K}\right)^2 + 1 < 0. \tag{11}$$

In that case, the local growth rate of instability is given by the relation

$$\mathrm{Im}\ \omega = K^2 \sqrt{-\left[1 + 2\left(\frac{\phi_0}{K}\right)^2 (g_0(1+4\alpha T^2)^{-1/2} + 2\chi\phi_0^2)\right]}. \tag{12}$$

For attractive (to which we restrict this study) two-body interatomic interaction, the relation (11) may be rewritten in the form

$$2|g_0|\left(\frac{\phi_0}{K}\right)^2 (1+4\alpha T^2)^{-1/2} > 4\chi\phi_0^2\left(\frac{\phi_0}{K}\right)^2 + 1. \tag{13}$$

Taking into account, in relation (13), the fact that $0<(1+4\alpha T^2)^{-1/2}\leq 1$, we obtain the result that the unstable modes exist for $\chi<\chi_c$, with $\chi_c=\frac{1}{2\phi_0^2}|g_0|$, and the corresponding wave numbers satisfy the condition

$$K < K_c \quad \text{where} \quad K_c = 2\sqrt{\chi_c - \chi}\,\phi_0^2. \tag{14}$$

We discuss three regimes in relation (13).

(i) For $\chi\geq\chi_c$, all the modes are expected to be modulationally stable.

(ii) For $\chi\in[0,\chi_c[$, in the case $\alpha\neq 0$ and for unstable modes corresponding to (14), the modulational instability may develop during a time scale: $T<T_c=\frac{1}{2\sqrt{\alpha}}\frac{\sqrt{(\chi_c-\chi-Q^2)(\chi_c+\chi+Q^2)}}{\chi+Q^2}$; where $Q^2=\frac{K^2}{4\phi_0^4}$. Such a time scale corresponds, in terms of the physical variable t, to

$$t < t_c = \frac{1}{2\sqrt{\alpha}}\arccos\left(\frac{K^2+4\chi\phi_0^4}{4\chi_c\phi_0^4}\right). \tag{15}$$

(iii) For $\chi<0$, for unstable modes $K>K_s$ (with $K_s=2\sqrt{|\chi|}\phi_0^2$) obeying the condition (14), the modulational instability may develop during the time scale $t<t_c$ and for unstable modes $K\leq K_s$ it may set in early. The analytical treatment of the critical time t_c as a function of wave number K, trapping parameter α, and quintic nonlinearity coefficient χ leads to the following observations (Fig. 1). From relation (15), it is obvious that, for $\chi\geq\chi_c$, t_c is undefined for every wave number and every trapping parameter. In Fig. 1(a), $\chi\in[-\chi_c,\chi_c[$, t_c decreases as a function of K until $K=K_c$ (moreover, for the same K, it decreases when χ or α, see Fig. 1(c)), where it becomes nil [see Fig. 1(a)]. t_c is undefined for values of K higher than K_c. We note that K_c decreases when χ increases. In Fig. 1(b), $\chi<-\chi_c$, the graph $t_c=f(K)$ for any value of the trapping parameter presents an inflection point at $K=K_s$. t_c is undefined for increasing wave number until a particular value $K_c'=2\sqrt{-\chi_c-\chi}\phi_0^2$, where it takes a nonzero value (that value decreases when the trapping parameter increases). Then t_c decreases (with an inflection point at $K=K_s$) when the wave number increases from the particular value K_c' to the particular value K_c. For $K=K_c$, t_c takes the value zero and is undefined for values of K higher than K_c [see Fig. 1(b)]. Let us note that, when χ increases, K_c' and K_c decrease, in contrast to the difference $\Delta K_c=K_c-K_c'$.

Figure 2 shows the regions of MI obtained from the analytical study. In this figure, we plot the wave numbers $K_c=2\sqrt{\chi_c-\chi}\phi_0^2$ and $K_s=2\sqrt{|\chi|}\phi_0^2$ as functions of the quintic nonlinearity parameter χ; we therefore obtain three zones of instability and stability in the plane (χ,K). For a point (χ,K) taken in zone I, the MI may develop as soon as the experiment begins. In zone II the MI may develop during the time scale $t<t_c$. For the last zone (IIIa and IIIb) the system is expected to be modulationally stable. Waves are stable at every time in IIIb and just for a critical time $t_s=\frac{1}{2\sqrt{\alpha}}\arccos(\frac{K_c}{K})$ for IIIa. The critical time t_s is derived by realizing that the effective wave number of the initial perturbation (16) is $K|\cos(2\sqrt{\alpha}t)|$ rather than K, on account of the (modified) lens-type transformation. It should be noted that the existence of the three zones is due to the simultaneous consideration of the cubic-quintic nonlinearities. When the

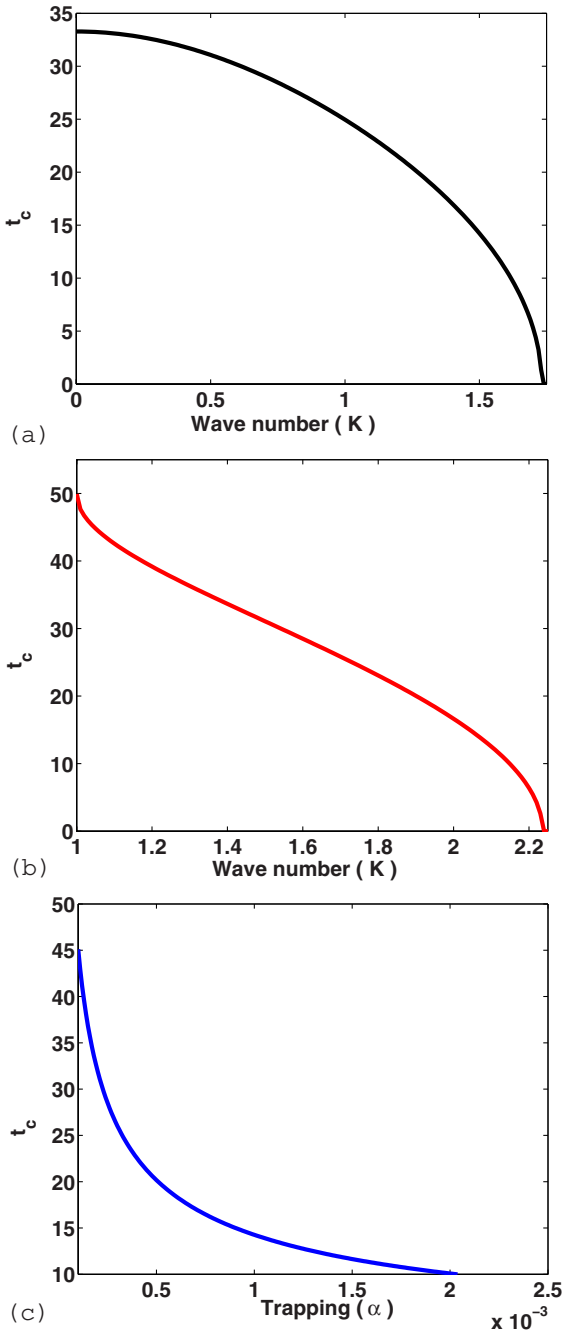

FIG. 1. (Color online) Variation of the critical time scale versus the wave number and trapping parameter. The parameters used are (a) $\alpha=0.001$, $\chi=-0.25$ ($\chi\in[-\chi_c,\chi_c[$, with $\chi_c=0.5$); (b) $\alpha=0.001$, $\chi=-0.75$ ($\chi<-\chi_c$); (c) $K=0.50$, $\chi=0.25$.

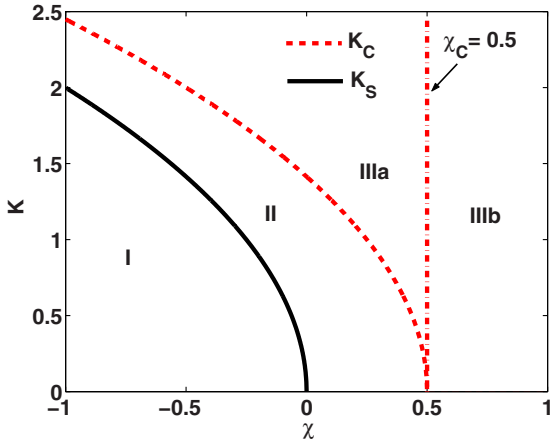

FIG. 2. (Color online) Regions of modulational stability and instability in the (χ, K) plane. The parameters used are $g_0=-1$; $\phi_0=1$.

two-body interaction is switched off, the zone II disappears. But, when the three-body interaction is neglected the instability-stability diagram in Fig. 2 merely reduces to the line $\chi=0$.

As noted in Ref. [25], it has also been verified here that external trapping (via α) enhances the instability, and the instability occurs at a short time scale for stronger trapping [see Fig. 1(c)]. Some interesting results emerge from our analysis.

In particular, in the absence of the quintic nonlinearity, unstable modes must always exist due to the cubic nonlinearity [see Eq. (14)]. Moreover, when the quintic nonlinearity is taken into account, the MI may appear or not, depending on the value of the coefficient χ (in the presence or absence of the cubic nonlinearity, controllable by the Feshbach resonance technique). However, the absence of the cubic nonlinearity in this case leads the system to have only attractive three-body interactions, while its presence permits the system to admit both attractive and repulsive three-body interactions. Thus the simultaneous presence of the cubic and quintic nonlinearities plays a very important role in the understanding of the diversified behaviors of BECs. The quintic nonlinearity provides also the possibility to control the domain of unstable modes. It also softens the destabilizing effects of external trapping and the cubic nonlinearity parameters.

Demonstrations of MI span a diverse set of disciplines ranging from fluid dynamics and plasma physics to nonlinear optics. In the context of nonlinear optics, MI has been examined using the generalized NLS equation with a nonlinear term of general form [34]. Therefore, in the framework of linear stability theory, we might also expected in the case of a BEC the same feature observed in nonlinear optics: the dynamics of beam propagation shows that beams with a slightly perturbed initial solution not only evolve to a perfect solitary beam but also lead to periodic oscillations of the amplitude [34,35].

III. NUMERICAL TREATMENT AND COMPARISON WITH ANALYTICAL RESULTS

To verify the MI conditions for BECs derived in the previous section, we perform direct numerical integrations of

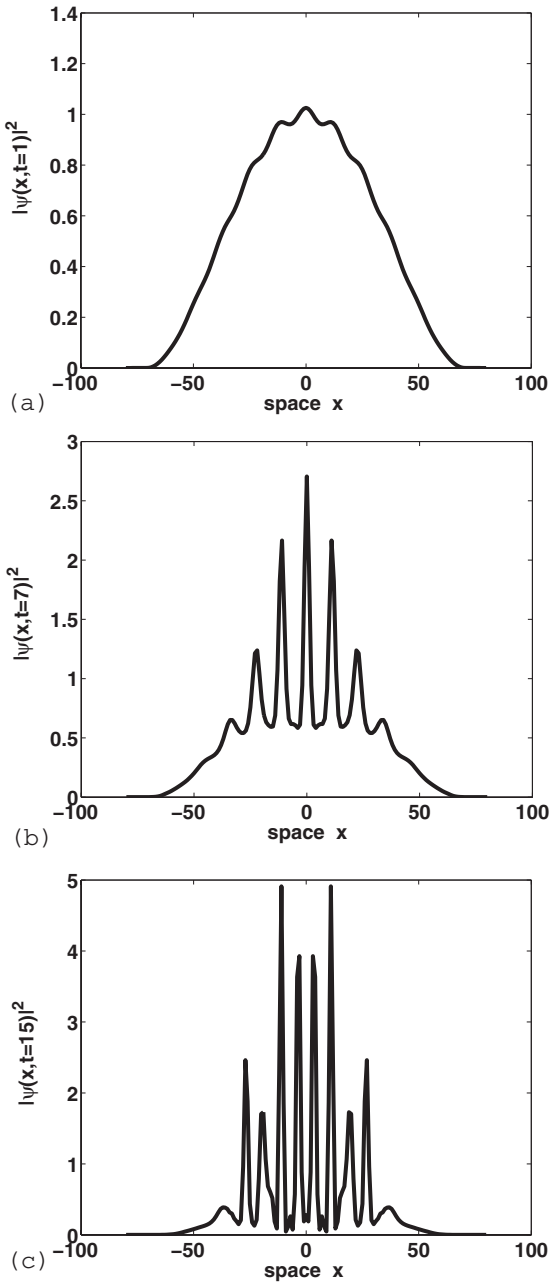

FIG. 3. Spatial evolution of modulated waves in term of solitary waves on top of the TF cloud, introducing the occurrence of the modulational instability, for weak trapping ($\alpha=0.0004$). The other parameters are $\chi=0.10$, $K=0.50$ (the point is located in zone II), and $t=$ (a) 1, (b) 7, and (c) 15.

the CQNLS equation (1). The initial condition used is

$$\psi(x,0) = \psi_{\mathrm{TF}}(\phi_0 + \varepsilon \cos(Kx)), \tag{16}$$

where $\psi_{\mathrm{TF}}=\sqrt{\max[0;1-V(x)]}$ is the background wave function in the Thomas-Fermi (TF) approximation. In a region close to the center $x=0$ and for convenient values of the potential, $\psi_{\mathrm{TF}} \simeq 1-\frac{1}{2}V(x)=1-\frac{1}{2}\alpha x^2$ [25,30]. In all numerical simulations, we have taken $\phi_0=1$, $g_0=-1$, and $\varepsilon=0.01$ (small compared to ϕ_0). Fixed boundary conditions are used.

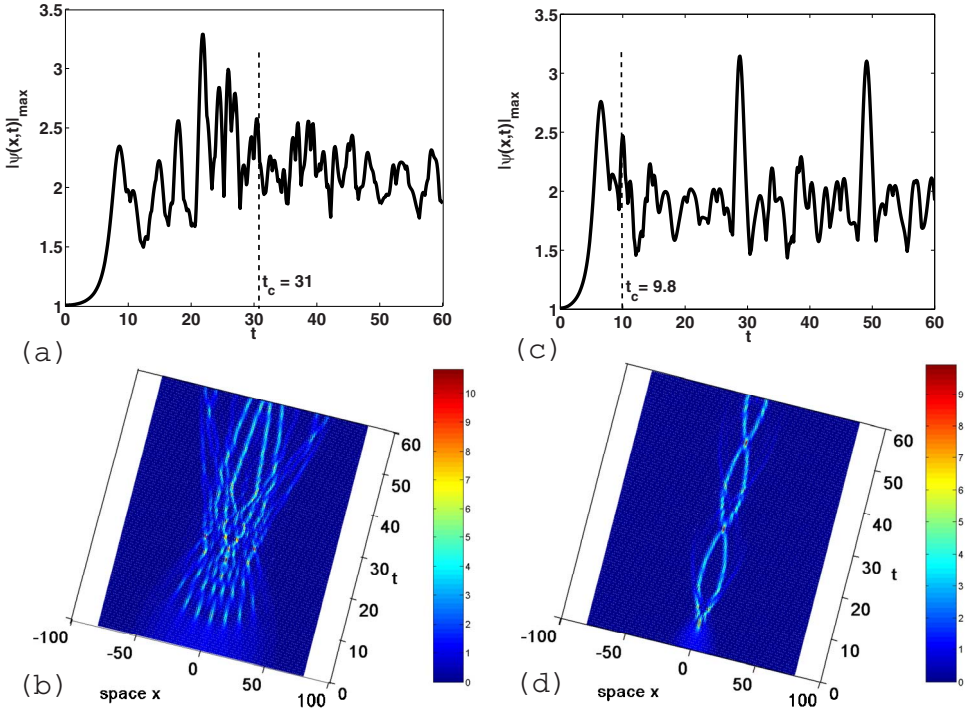

FIG. 4. (Color online) Spatiotemporal evolution of the maximum amplitude of the waves through the system, showing the modulational instability for different trappings. The parameters are $\chi=0.10$ and $K=0.50$ (the point used here is taken in zone II). (a) $|\psi(x,t)|_{\max}$ for $\alpha=0.0004$ (weak trapping). (b) $|\psi(x,t)|^2$ for $\alpha=0.0004$ (weak trapping). (c) $|\psi(x,t)|_{\max}$ for $\alpha=0.004$ (strong trapping). (d) $|\psi(x,t)|^2$ for $\alpha=0.004$ (strong trapping).

Most of the simulations are made with a space extending from $x=-80$ to 80.

Now, to illustrate our theoretical predictions, let us launch solution (16) through the system. For a point in zone II, the MI is predicted by the analytical study. Figure 3 depicts the spatial evolution of a modulated envelope solitary wave on top of the TF cloud $[|\psi(x,t)|^2]$. The initial wave [Fig. 3(a)] breaks up into a pulse chain [Fig. 3(b) at $t=7$ and Fig. 3(c) at $t=15$] as the time increases. That gives a proof of the development of MI in the system. We note that, while the width of each pulse decreases, the magnitude of the pulse increases. The number of pulses in the chain increases too. Figure 4 shows the time evolution of the maximal amplitude $[|\psi(x,t)|_{\max}]$ in Figs. 4(a) and 4(c); and the spatiotemporal evolution of the modulated envelope $|\psi(x,t)|^2$ in Figs. 4(b) and 4(d) for two different values of the trapping parameter. By comparing Figs. 4(a) and 4(c) we realize that, for the strong trapping case in Fig. 4(c), the instability sets in earlier. The theoretical time scales for the two cases, $t_c=31$ and 9.8, respectively, are numerically recovered during simulations. So the trapping enhances the instability. From Fig. 5, the same results are observed; the theoretical time scale is t_c

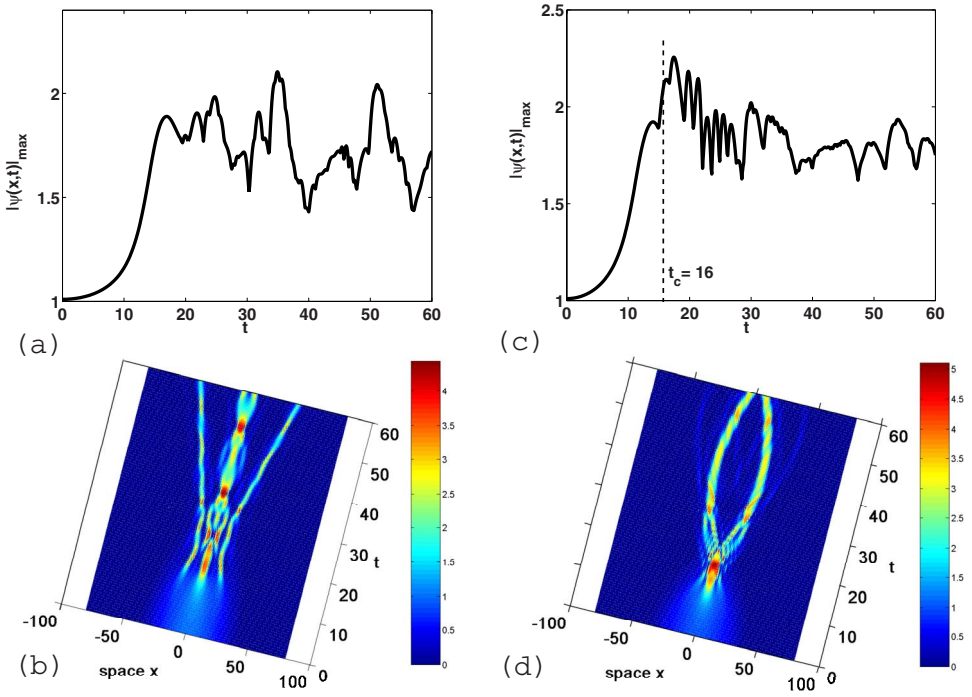

FIG. 5. (Color online) Spatiotemporal evolution of the maximum amplitude, showing the influence of the presence of the trapping on modulational instability, for the parameters $\chi=0.25$ and $K=0.25$ (a point of zone II). (a) $|\psi(x,t)|_{\max}$ for $\alpha=0$ (trapping turned off). (b) $|\psi(x,t)|^2$ for $\alpha=0$ (trapping turned off). (c) $|\psi(x,t)|_{\max}$ for $\alpha=0.001$ (trapping turned on). (d) $|\psi(x,t)|^2$ for $\alpha=0.001$ (trapping turned on).

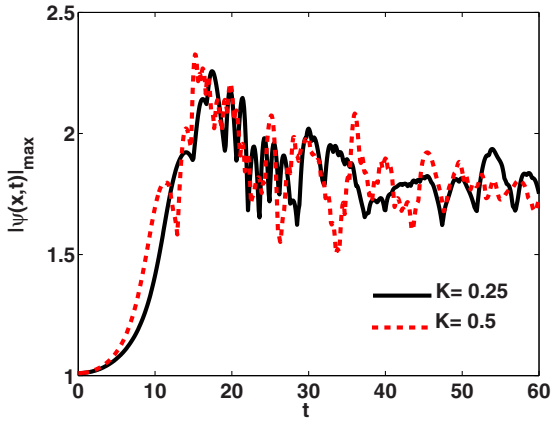

FIG. 6. (Color online) Time evolution of the maximum modulus of the waves $[|\psi(x,t)|_{\max}]$ through the system, showing the decrease of time scale when the wave number increases, for two wave numbers $K=0.25$ and 0.50 corresponding to points located in zone II. The other parameters are $\chi=0.25$ and $\alpha=0.001$.

$=16$ while the computational one is approximately $t_c=18$. But there is a more interesting aspect when the trapping is completely turned off [Fig. 5(a)]. The difference between Fig. 5(a) and Fig. 5(c) resides in the fact that, in the limit $\alpha=0$, we can only obtain $T=t$, as given by the lens-type transformation, such that Eqs. (1) and (3) are simply equivalent. According to that transformation, $T_c=\frac{1}{2\sqrt{\alpha}}\tan(2\sqrt{\alpha}t_c)$. So the case $t_c=18$ corresponds to $T_c=34.3$, when $\alpha=0.001$; which is in agreement with the numerical observations in Figs. 5(a) and 5(b). We remark that, for modulationally unstable modes launched with (16), the chain of pulses is made of two symmetric trains [Figs. 3(c) and 4(d)]. When the trapping $\alpha\neq 0$, the wave trains oscillate during the propagation in opposite directions and around $x=0$, with frequency close to $\frac{2\sqrt{\alpha}}{\pi}$ [see Figs. 4(d), 5(d), and 9(b)]. So the trains of solitons strongly attract and trap each other and subsequently propagate together as a bound state exhibiting transverse

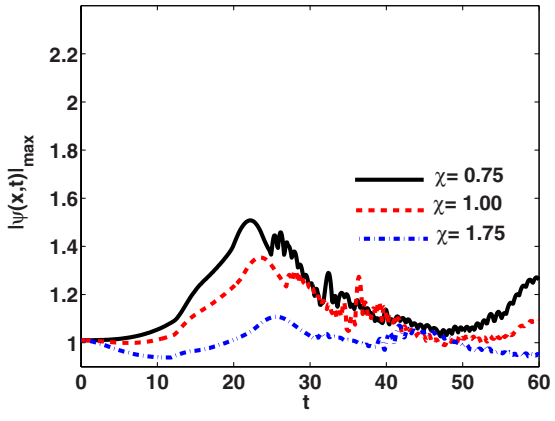

FIG. 7. (Color online) Stabilization of the system by the quintic nonlinearity: the time evolution of the maximum modulus of the waves $[|\psi(x,t)|_{\max}]$ through the system, for three values of the quintic parameter $\chi=0.75$, 1.00, and 1.75, corresponding to points located in zone IIIb. The other parameters are $K=0.25$ and $\alpha=0.001$.

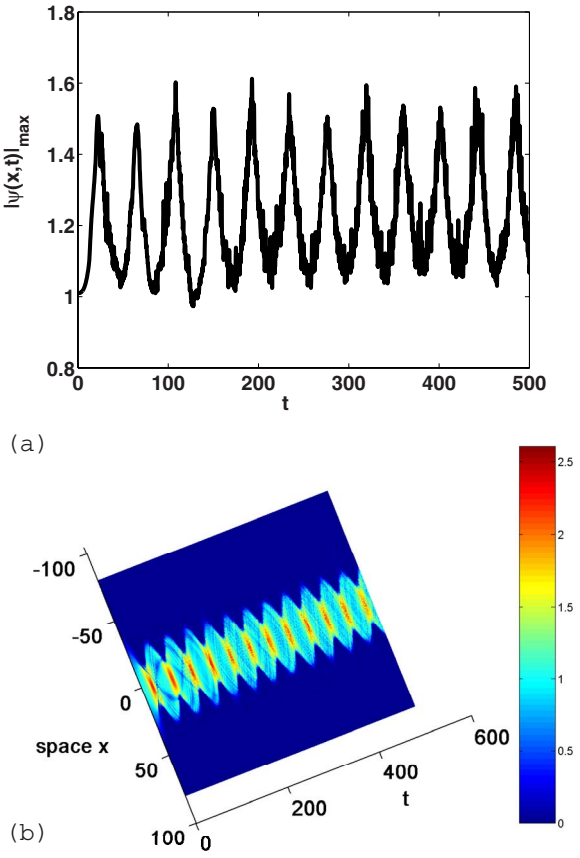

FIG. 8. (Color online) Recurrence phenomenon of the system stabilized by the quintic nonlinearity. It is seen through the evolution of a stable mode (the point used here is chosen in zone IIIb) for the quintic parameter $\chi=0.75$ and during a long period $t=500$. The other parameters are $K=0.25$ and $\alpha=0.001$. (a) The time evolution of the maximal modulus of the waves $[|\psi(x,t)|_{\max}]$ through space. (b) 3D view of the square modulus of the waves $[|\psi(x,t)|^2]$ through space and time.

oscillations. Figure 6 illustrates the time evolution of the modulated maximum amplitude for different perturbation wave numbers. This figure indicates that the development of MI depends on the perturbation wave number.

In region IIIb, the system is predicted to be modulationally stable. Let us consider the BEC with parameters of Fig. 5(c) but with χ increased to 0.75, 1.00, and 1.75, respectively. Figure 7 displays results obtained from the numerical simulations with these parameters. One can see that, as the quintic parameter increases, the magnitude of the waves decreases. Despite the trapping and the cubic nonlinearity, which is known to be destabilizing, the stability here can be obtained due to the quintic nonlinearity. Indeed, many works have already pointed the fact that the quintic nonlinearity can be used to stabilize a system [36,37]: Soto-Crespo *et al.* [36,37] studied the cubic-quintic Ginzburg-Landau equation having several exact soliton solutions in mind. However, by numerical study, they found that solitons are unstable in the model where the highest nonlinearity is cubic. Quintic terms have to be added to the system to obtain stable localized solutions. The present study also shows the usefulness of the quintic nonlinear term in a BEC. The BEC undergoes, for a

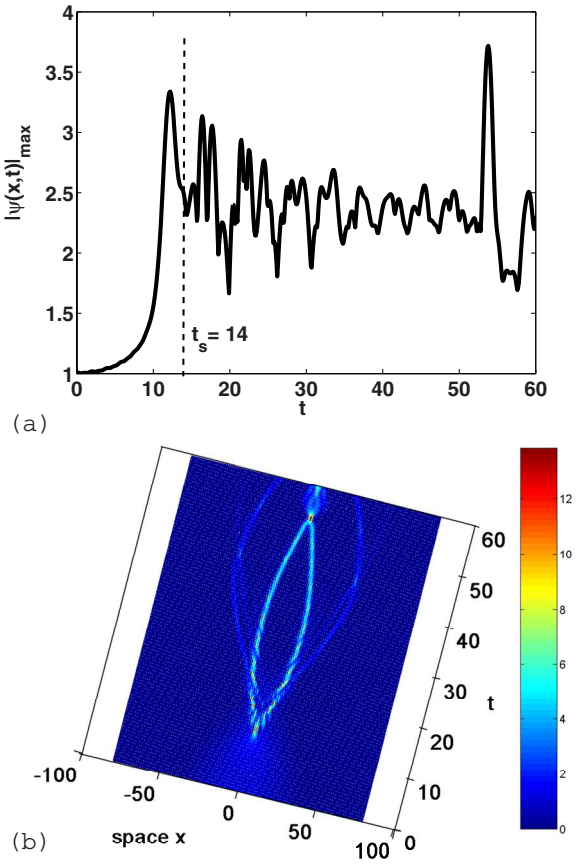

FIG. 9. (Color online) Rise of instability in an initially stable mode. The parameters are $\chi=0.10$ and $K=2.00$ (corresponding to a point of zone IIIa) and $\alpha=0.001$. (a) The time evolution of the maximal modulus of the waves $[|\psi(x,t)|_{\max}]$ through space. (b) 3D view of the square modulus of the waves $[|\psi(x,t)|^2]$ through space and time.

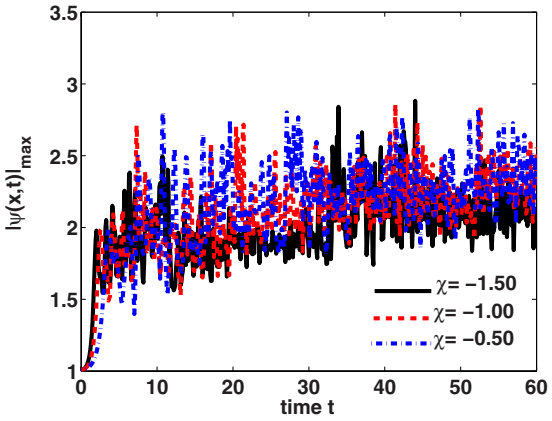

FIG. 10. (Color online) Modulational instability of three points picked in zone I. The time evolution of the maximum modulus of the waves $[|\psi(x,t)|_{\max}]$ through the system for a mode predicted to be initially unstable is shown for three values of the quintic parameter $\chi=-1.50$, 1.00, and −0.50 (corresponding to points of zone I). The other parameters are $K=1.00$ and $\alpha=0.001$.

long period, the recurrence phenomenon plotted in Fig. 8 for $\chi=0.75$. That phenomenon consists of benign oscillations that do not move the wave magnitude away from its initial value $\phi_0=1.0$.

A point in domain IIIa is also supposed to be stable but no longer after the critical time t_s theoretically given by $t_s=\frac{1}{2\sqrt{\alpha}}\arccos(\frac{K_c}{K})$. We choose $\chi=0.1$ and $K_c=1.265$. For the point (0.1,2) belonging to that domain, we present in Fig. 9 the time evolution of the maximum amplitude of the wave function. The instability is set in around $t_s=14$ as predicted analytically.

Finally, in zone I, let us pick three points $(-1.5,1)$, $(-1.0,1)$, and $(-0.5,1)$. Figure 10 depicts the time evolution of the maximum amplitude for these different points. We realize that the MI does not arise exactly at $t=0$. It occurs near the origin but after a time scale greater than 2. This may probably be related to the fact that solitary waves need a minimum time scale to develop.

Some of the phenomena found here have been reported previously for other physical systems. When the dynamics of the BEC is governed by the discrete nonlinear Schrödinger equation, intrinsically localized excitations, including discrete solitons and breathers, can be created [9,10,38]. In the context of the "traditional" NLS equation (without the external potential), perhaps the most standard mechanism through which bright solitons and solitary wave structures appears is through the activation of the MI of plane waves. In this case, the continuous wave solution of the NLS equation becomes unstable toward the generation of a chain of bright solitons. In this work we have shown that, under certain conditions, this may also happen in the case of the Gross-Pitaevskii equation with two- and three body interactions as well (see Figs. 3–5, 8, and 9).

IV. CONCLUSION

We have investigated, both analytically and numerically, the MI for a BEC with a harmonic potential. Using a modified lens-type transformation (in the limit of some restrictions), we have obtained time-dependent criteria for MI [relation (13)]. It should be noted that a modulationally unstable mode needs some time to develop into a solitary wave chain [relation (15)]. If a system does not have enough time, the solitary wave train structure will not appear. It is clear, as some studies have shown, that the three-body interatomic interaction term can play an important role. Hence, we have determined the MI domains as a function of the quintic term χ in the (χ,K) plane (Fig. 2). Thus, $\chi>\chi_c$ waves are stable at every time and no soliton will be generated (region IIIb). For $0<\chi<\chi_c$, two cases occur. The system is stable just for the critical time $t_s=\frac{1}{2\sqrt{\alpha}}\arccos(\frac{K_c}{K})$ (region IIIa). But the development of modulational unstable modes into a solitary wave chain will be effective during the time scale $t<t_c=\frac{1}{2\sqrt{\alpha}}\arccos(\frac{K^2+4\chi\phi_0^4}{4\chi_c\phi_0^4})$ (region II). In the case $\chi<0$, the MI may develop as soon as the experiment begins (region I). The analytical approach showed that the modulational instability is widely influenced by the quintic nonlinearity in addition to the cubic one.

We have used direct numerical simulations of the GP equation to prove the validity of our analytical predic-

tions, and excellent agreement is obtained. Numerical experiments have shown that, when the analytical predictions of the MI condition are satisfied, there is formation of localized pulses and wave trains. Our results also point out the crucial role of the simultaneous presence of two- and three-body interatomic interactions in the dynamics of BECs, as well as the importance of the external trapping parameter α.

[1] A. Griffin, D. W. Snoke, and S. Stringari, *Bose-Einstein Condensation* (Cambridge University Press, Cambridge, U.K., 1995).

[2] K. Huang, *Statiscal Mechanics*, 2nd ed. (Wiley, New York, 1987).

[3] D. N. Christodoulides and R. I. Joseph, Opt. Lett. **13**, 794 (1988); H. S. Eisenberg, Y. Silberberg, R. Morandotti, A. R. Boyd, and J. S. Aitchison, Phys. Rev. Lett. **81**, 3383 (1998).

[4] R. J. Chiao, F. Gardmire, and C. H. Townes, Phys. Rev. Lett. **13**, 479 (1964); P. Kelley, *ibid.* **15**, 1005 (1965).

[5] V. E. Zakharov, Zh. Eksp. Teor. Fiz. **62**, 1745 (1972); [Sov. Phys. JETP **35**, 908 (1972)].

[6] G. C. Papanicolaou, C. Sulem, P. L. Sulem, and X. P. Wang, Physica D **72**, 61 (1994).

[7] Yu. B. Gaididei, K. Ø. Rasmussen, and P. L. Christiansen, Phys. Rev. E **52**, 2951 (1995).

[8] M. A. Porter, M. Chugunova, and D. E. Pelinovsky, Phys. Rev. E **74**, 036610 (2006); G. Theocharis, D. J. Frantzeskakis, P. G. Kevrekidis, B. A. Malomed, and Y. S. Kivshar, Phys. Rev. Lett. **90**, 120403 (2003).

[9] L. Khaykovich *et al.*, Science **296**, 1290 (2002).

[10] F. Dalfovo, S. Giorgini, L. P. Pitaevskii, and S. Stringari, Rev. Mod. Phys. **71**, 463 (1999).

[11] H. Sakaguchi and B. A. Malomed, Phys. Rev. E **73**, 026601 (2006); S. K. Adhikari, New J. Phys. **5**, 137 (2003).

[12] W. Zhang, E. M. Wright, H. Pu, and P. Meystre, Phys. Rev. A **68**, 023605 (2003).

[13] F. Kh. Abdullaev, A. Gammal, L. Tomio, and T. Frederico, Phys. Rev. A **63**, 043604 (2001).

[14] N. Akhmediev, M. P. Das, and A. V. Vagov, Int. J. Mod. Phys. B **13**, 625 (1999); A. Gammal, T. Frederico, L. Tomio, and P. Chomaz, Phys. Rev. A **61**, 051602(R) (2000).

[15] C. Chin, T. Kraemer, M. Mark, J. Herbig, P. Waldburger, H. C. Nagerl, and R. Grimm, Phys. Rev. Lett. **94**, 123201 (2005).

[16] F. Kh. Abdullaev and M. Salerno, Phys. Rev. A **72**, 033617 (2005).

[17] G. L. Alfimov, V. V. Konotop, and P. Pacciani, Phys. Rev. A **75**, 023624 (2007).

[18] A. X. Zhang and J. K. Xue, Phys. Rev. A **75**, 013624 (2007).

[19] F. Cataliotti *et al.*, Science **293**, 843 (2001).

[20] H. Sakaguchi and B. A. Malomed, Phys. Rev. E **72**, 046610 (2005).

[21] F. Kh. Abdullaev, A. A. Abdumalikov, and R. M. Galimzyanov, Phys. Lett. A **367**, 149 (2007).

[22] B. P. Anderson, K. Dholakia, and E. M. Wright, Phys. Rev. A **67**, 033601 (2003).

[23] R. Kanamoto, H. Saito, and M. Ueda, Phys. Rev. A **67**, 013608 (2003).

[24] G. Theocharis, Z. Rapti, P. G. Kevrekidis, D. J. Frantzeskakis, and V. V. Konotop, Phys. Rev. A **67**, 063610 (2003).

[25] J. K. Xue, Phys. Lett. A **341**, 527 (2005); L. Wu and J. F. Zhang, Chin. Phys. Lett. **24**, 1471 (2007).

[26] Y. S. Kivshar and M. Peyrard, Phys. Rev. A **46**, 3198 (1992); A. Mohamadou, A. K. Jiotsa, and T. C. Kofane, Phys. Rev. E **72**, 036220 (2005).

[27] Z. Rapti, P. G. Kevrekidis, A. Smerzi, and A. R. Bishop, J. Phys. B **37**, S257 (2004).

[28] R. Lai and A. J. Sievers, Phys. Rev. B **57**, 3433 (1998).

[29] F. Kh. Abdullaev, J. G. Caputo, R. A. Kraenkel, and B. A. Malomed, Phys. Rev. A **67**, 013605 (2003).

[30] G. Théocharis, D. J. Frantzeskakis, P. G. Kevrekidis, R. Carretero-González, and B. A. Malomed, Math. Comput. Simul. **69**, 537 (2005).

[31] C. De Angelis, IEEE J. Quantum Electron. **30**, 818 (1994).

[32] B. V. Gisin, R. Driben, and B. A. Malomed, J. Opt. B: Quantum Semiclassical Opt. **6**, S259 (2004).

[33] E. B. Kolomeisky, T. J. Newman, J. P. Straley, and X. Qi, Phys. Rev. Lett. **85**, 1146 (2000).

[34] Y. S. Kivshar, D. Anderson, and M. Lisak, Phys. Scr. **47**, 679 (1993); F. Ndzana II, A. Mohamadou, and T. C. Kofane, Opt. Commun. **275**, 421 (2007).

[35] S. Gatz and J. Herrmann, J. Opt. Soc. Am. B **14**, 1795 (1997) and references therein.

[36] N. Akhmediev and A. Ankiewicz, in *Solitons of the Complex Ginzburg-Landau Equation*, edited by S. Trillo and W. E. Toruellas (Springer-Verlag, Berlin, 2001).

[37] J. M. Soto-Crespo, N. N. Akhmediev, V. V. Afanasjev, and S. Wabnitz, Phys. Rev. E **55**, 4783 (1997); J. M. Soto-Crespo, N. N. Akhmediev, and G. Town, Opt. Commun. **199**, 283 (2001); A. Mohamadou and T. C. Kofane, Phys. Rev. E **73**, 046607 (2006).

[38] S. Flach and C. R. Willis, Phys. Rep. **295**, 181 (1998).